

## Reflection and transmission properties of self-similar interfaces

Kees Wapenaar and Jacob Fokkema, Centre for Technical Geoscience, Delft University of Technology

### Summary

We represent an interface by a self-similar singularity, embedded between two homogeneous half-spaces and we evaluate its frequency-dependent normal incidence reflection and transmission coefficients. For  $f \rightarrow 0$  the expressions for the coefficients reduce to those for a discrete boundary between two homogeneous half-spaces; for  $f \rightarrow \infty$  the effect of the embedding half-spaces vanishes. These asymptotic expressions have a relatively simple form and depend on the singularity exponent  $\alpha$ .

Next we evaluate the time-domain reflection and transmission responses of a self-similar interface and of its smoothed version. It appears that smoothing has hardly any effect on the response, provided that the smoothing does not affect the scales corresponding to the seismic frequency range.

### Introduction

We parameterize an interface by the following singular function for the  $P$ -wave velocity:

$$c(z) = \begin{cases} c_1 |z/z_1|^{-\alpha_1} & \text{for } z < 0 \\ c_2 |z/z_2|^{\alpha_2} & \text{for } z > 0 \end{cases} \quad (1)$$

(the mass density will be parameterized as a step-function from  $\varrho_1$  to  $\varrho_2$  throughout this paper). When only one of the parameters  $\alpha_1$  and  $\alpha_2$  is not equal to zero we speak of a one-sided singularity; when both are non-zero the singularity is two-sided. For a two-sided singularity with  $\alpha_1 = \alpha_2 = \alpha$  it appears that the function in equation (1) is *self-similar*, according to  $c(\beta z) = \beta^\alpha c(z)$ , for  $\beta > 0$ . For  $\alpha_1 = \alpha_2 = 0$  this function reduces to the usual step-function.

|                                     | $z < 0$<br>(n=1) | $z > 0$<br>(n=2) |
|-------------------------------------|------------------|------------------|
| $c_n$ [m/s]                         | 800              | 1200             |
| $\varrho_n$ [kg/m <sup>3</sup> ]    | 1000             | 1000             |
| $z_n$ [m]                           | -5               | 5                |
| Two-sided:<br>$\alpha_n (= \alpha)$ | -0.4             | -0.4             |
| One-sided:<br>$\alpha_n$            | 0                | -0.4             |

Table 1. Parameter values, used in the examples in this paper.

For a two-sided singularity, with parameters  $\alpha$ ,  $c_n$  and  $z_n$  as defined in Table 1, the function  $c(z)$  as defined by equation (1) is shown in Figure 1a. We applied a multiscale analysis to this function, following the method described by Mallat and Hwang (1992) and Herrmann (1997). Figure 1b shows the continuous

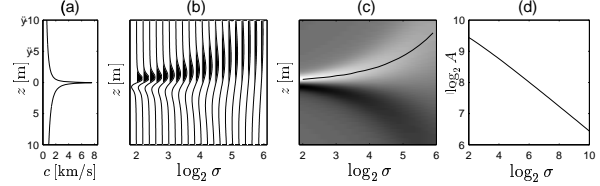


Fig. 1: (a) Two-sided self-similar velocity function, described by equation (1), with  $\alpha$ ,  $c_n$  and  $z_n$  defined in Table 1. (b) Continuous wavelet transform of the velocity function in figure a. (c) Modulus maxima line, obtained from figure b. (d) Amplitude-versus-scale (AVS) curve, measured along the modulus maxima line in figure c. The slope ( $\alpha = -0.4$ ) corresponds to the singularity exponent of the function in figure a.

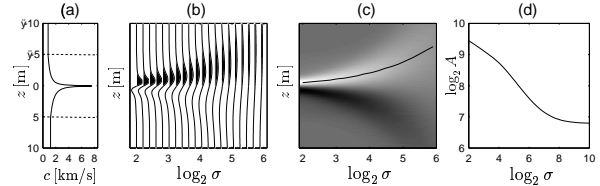


Fig. 2: Multi-scale analysis of the self-similar velocity function of Figure 1a, embedded between two homogeneous half-spaces  $z \leq z_1 = -5\text{m}$  and  $z \geq z_2 = 5\text{m}$ . For small  $\sigma$  the slope of the AVS curve in (d) is constant and again given by  $\alpha = -0.4$ ; for large  $\sigma$  the slope approaches zero, as for a step-function.

wavelet transform  $\tilde{c}(\sigma, z)$  of this function. In essence this result has been obtained by convolving  $c(z)$  with scaled versions of one and the same analyzing wavelet, i.e., with  $\frac{1}{\sigma}\psi(\frac{z}{\sigma})$  (this wavelet will be discussed in more detail in a later section). The different traces in Figure 1b correspond to different scales  $\sigma$ . Taking the modulus of the data in Figure 1b and connecting the local maxima from trace to trace, yields the so-called modulus maxima line that is shown in Figure 1c. Figure 1d shows the amplitudes measured along this line, on a log-log scale. The slope of this amplitude-versus-scale (AVS) graph corresponds to the singularity exponent  $\alpha = -0.4$  of the self-similar function in Figure 1a (Mallat and Hwang, 1992). Note that when this type of analysis would be applied to a step-function, the slope of the AVS curve would be zero.

The AVS behaviour, observed in Figure 1d, corresponds nicely to that of several outliers in real well-logs, as analyzed by Herrmann (1997). Although this ‘constant-slope’ behaviour is not universal, it makes sense to use functions of the form of equation (1) for the parameterization of composite reflectors. In this paper we will consider the situation in which a self-similar singularity is embedded between two homogeneous half-spaces. A multi-

## Reflection and transmission properties of self-similar interfaces

scale analysis of such an embedded singularity is shown in Figure 2. The singular function is defined in the region  $z_1 < z < z_2$  with the parameters of Table 1; the velocities of the embedding half-spaces are also given by  $c_1 = 800\text{m/s}$  and  $c_2 = 1200\text{m/s}$ , so that  $c(z)$  is continuous at  $z_1$  and  $z_2$ . Note that for small scales ( $\sigma \rightarrow 0$ ) the AVS curve in Figure 2d approaches that in Figure 1d. So in this limit the embedding half-spaces have no effect on the scaling behaviour. For large scales ( $\sigma \rightarrow \infty$ ) the AVS curve is nearly constant (as for a step-function), which implies that in this limit the scaling behaviour is fully determined by the embedding half-spaces.

In the following sections we evaluate the normal incidence reflection and transmission properties of this type of self-similar interface. Since the results are exact, they may serve as a reference for approximate expressions for more general situations. For example, Dessing (1997) analyzes the response of another class of scale-dependent reflector models. For a symmetric self-similar singularity (without embedding half-spaces), his results are consistent with the high-frequency expressions in this paper.

For the oblique incidence response no explicit expressions have been found yet (except for  $\alpha = 0$  and  $\alpha = -\frac{1}{2}$ ). However, by exploiting the self-similarity property  $c(\beta z) = \beta^\alpha c(z)$ , it is possible to derive self-similarity relations for the angle-dependent reflection and transmission coefficients. A further discussion of these extensions is beyond the scope of this paper.

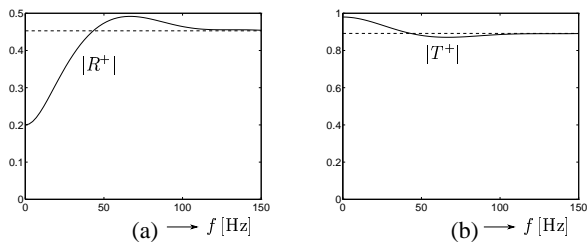


**Fig. 3:** Modulus of the reflection (a) and transmission (b) coefficients of the embedded two-sided singularity of Figure 2a (solid) and their high-frequency approximations (dashed).

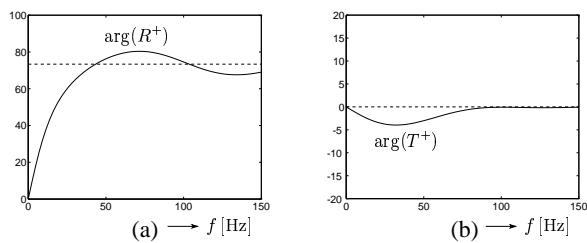


**Fig. 4:** Phase of the reflection (a) and transmission (b) coefficients of the embedded two-sided singularity of Figure 2a (solid) and their high-frequency approximations (dashed).

## Reflection and transmission coefficients

The exact reflection and transmission coefficients for a self-similar singularity, embedded between two homogeneous half-spaces, are derived in Wapenaar (1998). Here we consider the embedded two-sided singularity of Figure 2a, with  $\alpha$ ,  $c_n$ ,  $\varrho_n$  and  $z_n$  defined in Table 1. In Figures 3 and 4 the modulus and phase of  $R^+$  and  $T^+$  are shown as a function of the frequency. The low- and high-frequency limits will be discussed in the next two sections.

### Zero-frequency limit

For two-sided as well as one-sided singularities, embedded between two homogeneous half-spaces, the limits for  $f \rightarrow 0$  of the reflection and transmission coefficients  $R^\pm$  and  $T^\pm$  are given by

$$R^+ = -R^- \rightarrow \frac{\varrho_2 c_2 - \varrho_1 c_1}{\varrho_2 c_2 + \varrho_1 c_1}, \quad (2)$$

$$T^+ = T^- \rightarrow \frac{2\sqrt{\varrho_2 c_2 \varrho_1 c_1}}{\varrho_2 c_2 + \varrho_1 c_1} = \sqrt{1 - (R^+)^2}. \quad (3)$$

Note that these coefficients are equal to the flux-normalized coefficients for a discrete boundary between two homogeneous half-spaces, i.e., for the situation in which the velocity and density are described by step-functions. This is consistent with the multi-scale analysis in Figure 2, which revealed that for large  $\sigma$  the embedded self-similar singularity behaves as a step-function (bear in mind that the scale  $\sigma$  is proportional to the wavelength, hence,  $\sigma \rightarrow \infty$  corresponds to  $f \rightarrow 0$ ). For the values of  $c_n$  and  $\varrho_n$  in Table 1, equations (2) and (3) yield  $R^+ = -R^- \rightarrow 0.2$  and  $T^\pm \rightarrow \sqrt{0.96}$  (see Figure 3 for  $f \rightarrow 0$ ).

### High-frequency behaviour for two-sided singularities

For embedded two-sided singularities we take again  $\alpha_1 = \alpha_2 = \alpha$  (and  $|z_1| = |z_2|$ ). For this situation the limits for  $f \rightarrow \infty$  of the reflection and transmission coefficients  $R^\pm$  and  $T^\pm$  are given by

$$R^+ = -\{R^-\}^* \rightarrow j \left[ \frac{e^{-j\nu\pi} \varrho_2 c_2^{2\nu} + e^{j\nu\pi} \varrho_1 c_1^{2\nu}}{\varrho_2 c_2^{2\nu} + \varrho_1 c_1^{2\nu}} \right], \quad (4)$$

$$T^+ = T^- \rightarrow \frac{2 \sin(\nu\pi) \sqrt{\varrho_2 c_2^{2\nu} \varrho_1 c_1^{2\nu}}}{\varrho_2 c_2^{2\nu} + \varrho_1 c_1^{2\nu}}, \quad (5)$$

with  $\nu = 1/(2 - 2\alpha)$  and  $\alpha < \frac{1}{2}$ . Note that these asymptotic expressions are frequency-independent. The factor  $j$  in equation (4) corresponds to a Hilbert transform in the time domain. For  $c_n$ ,  $\varrho_n$  and  $z_n$  as defined in Table 1 and variable  $\alpha$ , the modulus and phase of the high-frequency reflection and transmission coefficients  $R^+$  and  $T^+$  are shown in Figure 5. For  $\alpha = -0.4$  we have  $|R^\pm| \rightarrow 0.4528$ ,  $\arg(R^+) \rightarrow 73.37^\circ$ ,  $\arg(R^-) \rightarrow 106.63^\circ$ ,  $|T^\pm| \rightarrow 0.8916$ ,  $\arg(T^\pm) = 0^\circ$ . These values (except  $\arg(R^-)$ ) are represented by the dashed lines in Figures 3 and 4. The coefficients in equations (4) and (5) are equal to the exact coefficients for a two-sided self-similar function described by equation (1), (i.e., without the embedding homogeneous half-spaces). This is consistent with the multi-scale

## Reflection and transmission properties of self-similar interfaces

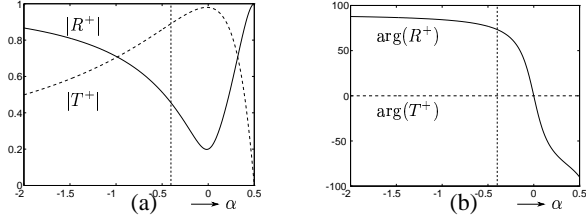


**Fig. 5:** High-frequency approximation of the modulus (a) and phase (b) of the reflection coefficient  $R^+$  (solid) and the transmission coefficient  $T^+$  (dashed) of an embedded two-sided singularity. The moduli and phases are plotted as a function of the singularity exponent  $\alpha$ ; the parameters  $c_n$ ,  $\varrho_n$  and  $z_n$  are defined in Table 1. For  $\alpha = -0.4$  the moduli and phases correspond to those in Figures 3 and 4 for  $f \rightarrow \infty$ .

analysis in Figures 1 and 2, which revealed that for small  $\sigma$  the embedding half-spaces have no effect on the scaling behaviour of the singularity (bear in mind that  $\sigma \rightarrow 0$  corresponds to  $f \rightarrow \infty$ ). At this point it is useful to give a quantitative interpretation of the scales  $\sigma$  along the horizontal axes in these figures. As we mentioned in the introduction, the multiscale analysis involves a convolution with a scaled wavelet  $\frac{1}{\sigma} \psi(\frac{z}{\sigma})$ . The wavelet that was used in Figures 1 and 2 is the derivative of a Gaussian, defined as

$$\psi\left(\frac{z}{\sigma}\right) = \frac{\partial}{\partial z} \left[ \frac{\exp\left[-\left(\frac{z}{2\sigma\Delta z}\right)^2\right]}{2\sqrt{\pi}} \right], \quad (6)$$

with  $\Delta z = 0.1$  m. The Fourier transform of this wavelet is  $j(k\sigma\Delta z)\exp[-(k\sigma\Delta z)^2]$  and reaches its maximum at  $k_0 = 1/(\sigma\Delta z\sqrt{2})$ . Hence, the effective wavelength of the analyzing wavelet is given by  $\lambda_{\text{eff}} = 2\pi/k_0 = 2\sqrt{2}\pi\sigma\Delta z$ , from which we derive that  $\log_2\sigma = \{2, 4, 6, 8, 10\}$  corresponds to  $\lambda_{\text{eff}} = \{3.5, 14, 57, 228, 910\}$  m. Unfortunately these wavelengths can not be uniquely related to seismic frequencies, since the velocity is not constant. Using an effective velocity  $c_{\text{eff}}$  we define the corresponding effective seismic frequency as  $f_{\text{eff}} = \frac{c_{\text{eff}}}{\lambda_{\text{eff}}}$ . Choosing (quite arbitrary)  $c_{\text{eff}} = 2000$  m/s, we thus find that the aforementioned range of scales corresponds to  $f_{\text{eff}} = \{570, 142, 34, 9, 2.2\}$  Hz. Hence, the scales  $\log_2\sigma = 4$  to  $\log_2\sigma = 8$  roughly correspond to the seismic scale range. In Figures 1d and 2d we observe that the AVS curves of the velocity functions in Figures 1a and 2a match very accurately for scales smaller than the seismic scales; within the seismic scale range they follow a similar trend and for larger scales they are completely different. Hence, the high-frequency approximations given by equations (4) and (5) are very accurate for frequencies above the seismic frequency range. How well they perform within the seismic frequency range will be investigated with an example in a later section.

### High-frequency behaviour for one-sided singularities

For embedded one-sided singularities we take  $\alpha_1 = 0$  and  $\alpha_2 \neq 0$ . For this situation the limits for  $f \rightarrow \infty$  of the reflecion and

transmission coefficients  $R^\pm$  and  $T^\pm$  are given by

$$R^+ \rightarrow \frac{\frac{\Gamma(\nu)}{\Gamma(1-\nu)}(j\omega\nu|z_2|)^{1-2\nu}\varrho_2c_2^{2\nu} - \varrho_1c_1}{\frac{\Gamma(\nu)}{\Gamma(1-\nu)}(j\omega\nu|z_2|)^{1-2\nu}\varrho_2c_2^{2\nu} + \varrho_1c_1}, \quad (7)$$

$$R^- \rightarrow \frac{-\frac{\Gamma(\nu)}{\Gamma(1-\nu)}(\omega\nu|z_2|)^{1-2\nu}\varrho_2c_2^{2\nu} + j^{1-2\nu}\varrho_1c_1}{\frac{\Gamma(\nu)}{\Gamma(1-\nu)}(j\omega\nu|z_2|)^{1-2\nu}\varrho_2c_2^{2\nu} + \varrho_1c_1}, \quad (8)$$

$$T^\pm \rightarrow \frac{\frac{2\sqrt{\pi}}{\Gamma(1-\nu)}\sqrt{(j\omega\nu|z_2|)^{1-2\nu}\varrho_2c_2^{2\nu}\varrho_1c_1}}{\frac{\Gamma(\nu)}{\Gamma(1-\nu)}(j\omega\nu|z_2|)^{1-2\nu}\varrho_2c_2^{2\nu} + \varrho_1c_1}, \quad (9)$$

with  $\omega = 2\pi f$ ,  $\nu = 1/(2 - 2\alpha_2)$  and  $\alpha_2 < \frac{1}{2}$ . Note that these asymptotic expressions are frequency-dependent, unlike the coefficients in equations (4) and (5) for the two-sided singularity. The factors  $(j\omega)^{1-2\nu}$  correspond to a fractional differentiation or integration in the time domain for negative and positive  $\alpha_2$ , respectively.

For  $\alpha_2$ ,  $c_n$ ,  $\varrho_n$  and  $z_n$  as defined in Table 1, the modulus and phase of the high-frequency reflection and transmission coefficients  $R^+$  and  $T^+$  are shown in Figure 6.

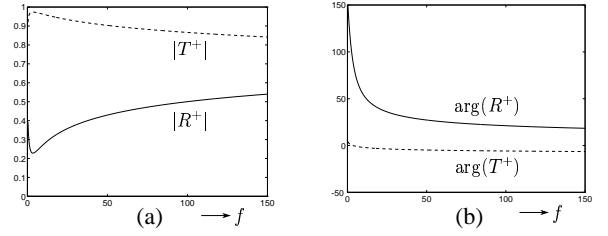


**Fig. 6:** High-frequency approximation of the modulus (a) and phase (b) of the reflection coefficient  $R^+$  (solid) and the transmission coefficient  $T^+$  (dashed) of an embedded one-sided singularity, for the parameters defined in Table 1.

### Reflection and transmission responses

In this section we consider the time-domain reflection and transmission responses of the embedded two-sided singularity shown in Figure 2a. For the downgoing incident wave field we choose a Ricker wavelet, defined by  $s_R(t) = (1 - 2\pi^2 f_0^2 t^2) e^{-\pi^2 f_0^2 t^2}$ , with  $f_0 = 50$  Hz. The Fourier transform of this wavelet is  $S_R(f) = \frac{2}{\sqrt{\pi}} \frac{f^2}{f_0^3} e^{-f^2/f_0^2}$ . Multiplying this spectrum with the exact complex reflection and transmission coefficients of Figures 3 and 4 and transforming the results back to the time-domain yields the reflection and transmission responses, shown by the solid lines in Figure 7. Note that in the reflection response a significant phase distortion of the Ricker wavelet is observed, in agreement with Figure 4a. The transmission response, on the other hand, has undergone nearly no phase distortion, in agreement with Figure 4b. Figure 7 also shows the high-frequency approximations of the reflection and transmission responses, denoted by the crosses (+). These responses have been obtained using the asymptotic reflection and transmission coefficients of

## Reflection and transmission properties of self-similar interfaces

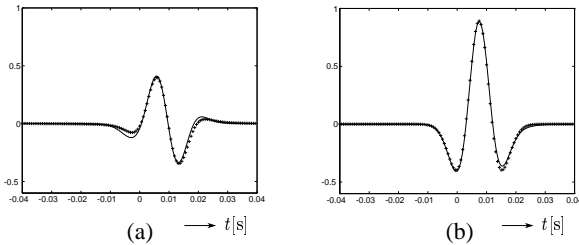


**Fig. 7:** Reflection (a) and transmission (b) responses of the embedded two-sided singularity of Figure 2a (solid) and their high-frequency approximations (+).

Figure 5 (for  $\alpha = -0.4$ ). Note that the main features of the exact responses are reasonably well reproduced by these high-frequency approximations.

### The effect of singularity smoothing

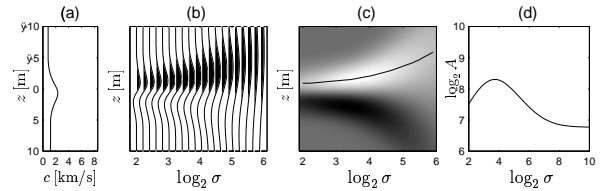
Due to the band-limited nature of a seismic source, only a limited range of scales of an interface will affect its reflection and transmission responses. In particular, removing small scales by smoothing the singularity will only have a small effect on these responses. In this section we investigate this effect with a numerical experiment.

Figure 8a shows a smoothed version of the previously considered self-similar interface of Figure 2a. Figure 8b shows a multiscale analysis of this smoothed interface. Comparing the AVS curve of Figure 8d with that of the original interface (Figure 2d) reveals that in the seismic scale range ( $\log_2 \sigma = 4$  to  $\log_2 \sigma = 8$ ) these AVS curves do not deviate significantly. Hence, we may expect that the smoothing has not much effect on the seismic reflection and transmission responses.

The numerically modeled responses of the smoothed interface in Figure 8a are represented by the crosses (+) in Figure 9; the solid lines in this figure are again the exact responses of the unsmoothed interface. Indeed the smoothing has hardly any effect on these responses.

### Conclusions

We have introduced a scale-dependent interface in which a self-similar singularity is embedded between two homogeneous half-spaces. A multiscale analysis revealed that for large scales ( $\sigma \rightarrow \infty$ ) this interface is indistinguishable from the usual step-function whereas for small scales ( $\sigma \rightarrow 0$ ) the scaling behaviour is dominated by the singularity. We have presented analytical results for the normal incidence reflection and transmission coefficients of this interface. These coefficients appear to be frequency-dependent. For small frequencies ( $f \rightarrow 0$ ) these coefficients reduce to the well-known coefficients of a step-function interface, whereas for large frequencies ( $f \rightarrow \infty$ ) the coefficients are equal to those of a singular function without the embedding half-spaces. For two-sided singularities these asymptotic coefficients are frequency-independent; the factor  $j$



**Fig. 8:** Multiscale analysis of a smoothed version of the interface of Figure 2a.

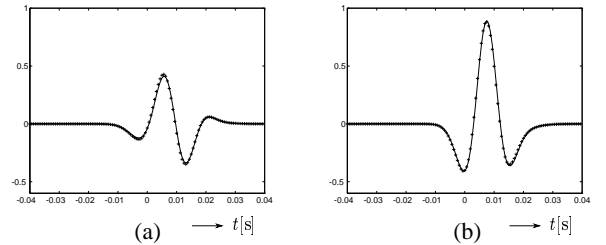


**Fig. 9:** Reflection (a) and transmission (b) responses of the embedded two-sided singularity of Figure 2a (solid) and of its smoothed version in Figure 8a (+).

in the expression for the reflection coefficient corresponds to a Hilbert transform in the time domain. For one-sided singularities the asymptotic coefficients are frequency-dependent; the factors  $(j\omega)^{1-2\nu}$  correspond to a fractional differentiation/integration in the time domain.

Using a numerical method we modeled the response of a smoothed version of the singularity. We showed that smoothing has hardly any effect on the response, provided that the smoothing does not affect the scales corresponding to the seismic frequency range.

Throughout this paper we have restricted ourselves to the normal incidence responses of one particular form of a self-similar interface. Since the results are exact, they may serve as a reference for approximate expressions that can handle more general situations.

### Acknowledgement

The authors would like to thank Frank Dessim and Jeroen Goudswaard for the fruitful discussions and for carrying out the multiscale analyses of the singular functions. This work is financially supported by the Dutch Technology Foundation (STW, grant DTN44.3547).

### References

- F. J. Dessim. *A wavelet transform approach to seismic processing*. PhD thesis, Delft University of Technology, 1997.
- F. J. Herrmann. *A scaling medium representation*. PhD thesis, Delft University of Technology, 1997.
- S. G. Mallat and W. L. Hwang. Singularity detection and processing with wavelets. *IEEE Trans. Inform. Theory*, 38(2):617–643, 1992.
- C. P. A. Wapenaar. Seismic reflection and transmission coefficients of a self-similar interface. *Geoph. J. Int.*, 135:585–594, 1998.